

# Decomposition of the cardiac and respiratory components from impedance pneumography signals

Marcel Młyńczak<sup>1</sup> and Gerard Cybulski<sup>1,2</sup>

<sup>1</sup>*Institute of Metrology and Biomedical Engineering, Faculty of Mechatronics, Warsaw University of Technology, Boboli 8, 02-525, Warsaw, Poland*

<sup>2</sup>*Department of Applied Physiology, Mossakowski Medical Research Centre, Polish Academy of Sciences, Pawinskiego 5, 02-106 Warsaw, Poland*  
{mlynczak, g.cybulski}@mchtr.pw.edu.pl

**Keywords:** ambulatory monitoring, impedance pneumography, cardiorespiratory activity, decomposition

**Abstract:** Impedance pneumography (*IP*) measures changes of thoracic electrical impedance connected with change of the air volume in the lungs. The electrode configuration used in *IP* applications causes that electrical heart activity is visible in the *IP* signals. The aim of this paper is to assess the opportunity to decompose both respiratory and cardiac components and its quality using various methods. Ten students performed static breathing sequences, intended both for calibration and testing. Our prototype, Pneumonitor 2, and the reference pneumotachometer, were used. The accuracy of calculating tidal volume and heart rate, the calibration procedure and the time of analysis, were considered. Mean 86.5% accuracy of tidal volume calculating and only 2.7% error of heart rate estimation were obtained using moving average smoothing filters, for simple short recording of free breathing calibration procedure, in three body positions. More sophisticated adaptive filtering also provided good accuracy, however the processing time was 100-times higher, compared to simple methods. It seems impedance pneumography, without *ECG*, could be enough for measuring basic cardiorespiratory activity, particularly during ambulatory recordings, in which the least disturbing equipment is desirable.

## 1 INTRODUCTION

### 1.1 Problem

In nowadays there is increasing number of conditions, when measuring respiration activity (*e.g.*, tidal volume, *TV*) could be necessary to improve the inference about training, diagnostics or even treatment. There is a strong need to perform such studies during natural functioning of the subjects, due to reliability of data gathered outside medical environment (Poupard et al., 2008; Koivumaki et al., 2012).

However, direct method, pneumotachometry (*PNT*), could not be reliably carried out outside the laboratory, due to its limitations (unportability and use of face mask). From that perspective a development of alternative methods, which could provide the possibility to measure ventilation can be visible (Houtveen et al., 2006; Młyńczak and Cybulski, 2012). One of those methods is impedance pneumography (*IP*), which measures changes of transthoracic electrical impedance, based on changes of amount of air in the lungs. It could be used both in laboratory

and ambulatory settings (Seppa et al., 2010; Seppa et al., 2013b).

The most common way of performing impedance measurements is tetrapolar method, in which two electrodes apply current signal and two remaining measure voltage, which is related to the electrical impedance. Various electrode configuration were studied and utilized, however usually voltage electrodes are positioned in the same place, on the midaxillary line at about 5th-rib level (Seppa et al., 2013a).

This setting is similar to the one used in ambulatory *ECG* recordings, where single first *ECG* lead configuration is applied. Shifting the placement from the chest to the midaxillary line might change the shape of the *ECG* signals, however it does not change the timing relationships between particular waves and cycles. Based on that, cardiac components were observed in the *IP* signals, because of the electrical, not mechanical, activity of the heart (Seppa et al., 2011). The sample raw *IP* signal, obtained during the preliminary measurements, is presented in the Figure 1.

In order to provide accurate respiratory parameters (particularly peak-related values, like *TV*, or

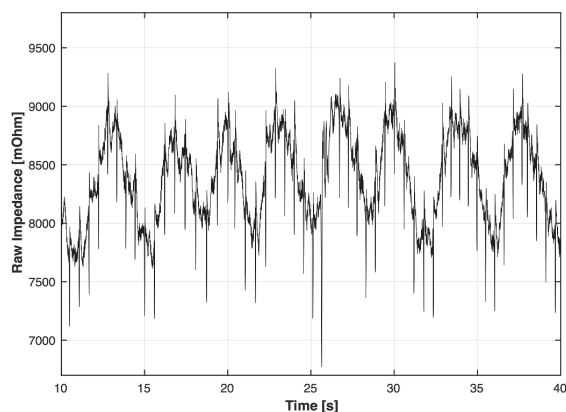


Figure 1: Sample of the raw *IP* signal consisting of both respiratory and cardiac components.

maximum flow during inspiration and expiration) these cardiac components should be removed and somehow ignored from the *IP* signal.

However, preprocessing methods could impact on the recorded signal. Firstly, by degrading the correspondence between respiratory *IP* component and reference signal in the areas of minimums and maximums of the signals. Secondly, due to the non-zero mean value of the cardiac component of the *IP* signal between the beginning of P wave and the ending of T wave, particularly caused by QRS cycle and T wave.

## 1.2 Related Work

The problem has already been observed in the past and some algorithms were used or introduced in the literature, as in the author's previous paper (Młyńczak et al., 2015).

Apart from simple filtration or moving average, Savitzky-Golay-related smoothing method was carried out, due to its well performance at minimums and maximums (Savitzky and Golay, 1964). For the graphical comparison the basic methods were applied on the sample raw *IP* signal and the outputs were showed in the Figure 2.

There are also more sophisticated approaches presented in the literature. Seppa et al. proposed the method to remove cardiac components adaptively based on simultaneous recording of *ECG*, which was inspired from Schuessler's work on removing cardiogenic oscillations from esophageal pressure signals (Seppa et al., 2011; Schuessler et al., 1998). Reinsch et al. and Schoenberg et al. suggested smoothing splines (Reinsch, 1967; Schoenberg, 1964; Poupard et al., 2008). Yasuda and Barros offered the method of filtering non-correlated noise in impedance cardiography, which could be applied for impedance pneu-

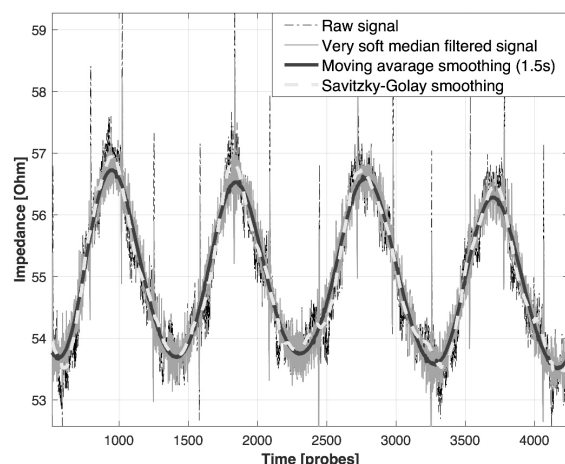


Figure 2: The comparison of basic filtration methods outputs applied on the sample raw *IP* signal.

mography too (Barros et al., 1995).

Empirical Modes Decomposition (*EMD*) and Ensemble Empirical Modes Decomposition (*EEMD*) were also evaluated, however the choice of modes, which are strictly related to respiratory activity, was not clear and trivial (Wang et al., 2016). From the other hand, wavelet denoising, based on different wavelets families, seems to be reliable tool to remove cardiac component in the *IP* signal as well (Mathworks, 2016).

Adaptive filtering and Scaled Fourier Linear Combiner (*SFLC*) was used by Yasuda et al. to assess obstructive sleep apnea and central hypopnea based on changes of thoracic impedance and *HRV* (Yasuda et al., 2005). Cardiac-related artefacts could be also attenuated during motion artefact removing process, presented in Ansari et al. work (Ansari et al., 2016).

However, it is worth noted, that cardiac-related component in the *IP* signal was usually treated as noise (Seppa et al., 2010), and still all mentioned algorithms intended to remove cardiac component from the *IP* signal, in order respiratory one to be as shape-connected to reference as it possible.

## 1.3 Objectives

Consequently, it seems important to evaluate whether there is the possibility to separate both components in *IP* signal and use both of them as valuable signals; respiratory component to calculate quantitative volume-, flow- and time-related parameters, and cardiac one to measure heart rate (*HR*), tachogram and heart rate variability (*HRV*) parameters.

Therefore, the aim of this paper is to assess the quality of various preprocessing methods, which

could be applied on raw *IP* signal in order to separate respiratory and cardiac components, concerning five aspects:

- What calibration procedure could provide the best data for further measurements?
- What are determination coefficients ( $R^2$ ) of the calibration model between respiratory component of *IP* to the reference for calibration data?
- What are inspiratory and expiratory tidal volumes ( $TV_{in}$  &  $TV_{ex}$ ) between respiratory component of *IP* to the reference for testing data?
- Is cardiac component subtracted from raw signal is comparable to the single-lead *ECG* signal in terms of *HR* and *HRV* calculation possibilities?
- What is the analysis duration and complexity?

The goal of the work is to indicate the most robust algorithm from both respiratory, and cardiac perspective. Different compromise approaches were discussed.

## 2 METHODS

### 2.1 Subjects & Devices

The participants of the study were 10 generally healthy students (all males, without any respiratory disease reported), who were informed about the aim of the study and wrote the consents.

The Table 1 presents the basic information about the study group.

Table 1: Information about the study participants.

	Minimum	Mean	Maximum
<b>Weight [kg]</b>	65.0	77.4	100.0
<b>Height [cm]</b>	171.0	179.3	187.0
<b>BMI</b>	20.75	24.14	33.41
<b>Age</b>	19	23	27

The Flow Measurement System with a Spirometer Unit M909 and a Fleisch-type Heatable Flow Transducer 5530, with a Conical Mouthpiece M9114 connected to the *PNT* sensor, was used without any resistance as a reference device, made by Medikro Oy (Kuopio, Finland). The system was calibrated with the 3L syringe to provide accurate flow values everyday.

*IP* signals were gained from our impedance pneumography prototype, Pneumonitor 2, which also enables to measure *ECG* signal and motion (from 3-axis accelerometer module). Single-lead *ECG* signal from

our prototype was treated as reference to analyze cardiac components extracted from *IP*.

Originally, sampling frequency of the reference device was  $200Hz$ , however due to the Pneumonitor 2 setting ( $f_s = 250Hz$ ), all signals were transformed (interpolated) to that sampling frequency.

### 2.2 Protocol & Analysis

The scheme of analysis is presented in the Figure 3.

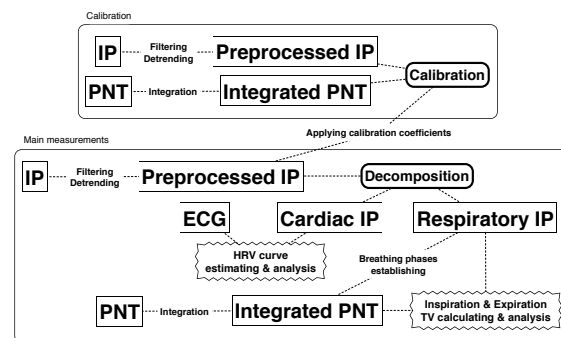


Figure 3: The scheme of analysis, distinguishing signals, operations and final analyses; the whole is performed for each body position separately.

In order to deal with first question marked in objective subsection, we proposed three types of calibration protocols, regarding time of registration and breathing regularity:

1. free breathing registered for 30 seconds, considered as the simplest and the quickest procedure, hereafter called '**Calibration Procedure 1**',
2. free breathing recorded for 2 minutes, to evaluate the impact of longer measurement, hereafter called '**Calibration Procedure 2**',
3. fixed breathing, shallow and deep alternately, 4 times each, for three frequencies, 6, 10 and 15 breaths per minute (BPM), to check, whether adding various rates and depths of breathing may improve the calibration quality meaningfully, hereafter called '**Calibration Procedure 3**'.

As we observed, body position has significant impact on the values of calibration coefficients provided for each subjects, therefore all 3 calibration procedure were performed in three body positions (supine, sitting and standing).

Finally, we asked to perform the test procedure consisting of 6 normal breaths and then 6 deep breaths (the difference was subjective), for three breathing rates (6, 10 and 15 BPM) and for three body positions (listed above). That data were also used to perform calibration (hereafter called '**Calibration Procedure 4**'), in order to evaluate the largest possible

accuracy, due to use of the same measurement both for calibration and for testing.

The reference breathing phases for each recording were calculated using simple amplitude thresholding of the flow-related raw *PNT* signal. Three states, inspiration, expiration and breathing pause, were automatically marked. Some heuristics were also added in order to remove the artefacts and very short phases and errors. Then, the volume-related reference signals were obtained by linearly detrended integration, using Simpson's rule, of pneumotachometry signal.

All *IP* signals (intended both for calibration and for testing purposes) were next processed by various techniques, listed below:

1. Moving average smoothing with 0.5 second window, considered as mild one.
2. Moving average smoothing with 1 second window, as proposed by *Koivumaki et al.* (Koivumaki et al., 2012).
3. Moving average smoothing with 1.5 second window, intended to be strong one.
4. Savitzky-Golay 2nd-order filter with 25 probes window (Savitzky and Golay, 1964).
5. Savitzky-Golay 7th-order filter with 25 probes window.
6. Subtraction of raw *IP* signal and the noise component from least mean square adaptive filtration, then smoothed by 200 ms window.
7. The same subtraction as in algorithm 6, however smoothed stronger, by 400 ms window.
8. The process of 25-fold decimation (performed twice using 5-fold coefficient), then applying 10th order least-square FIR filter with 1 Hz pass and 2.5 Hz stop frequencies, at the end the spline interpolation to return to original sampling frequency.
9. The same process as in algorithm 8, but use of 10th order stable Chebyshev IIR 1 Hz pass frequency filter.
10. Wavelet denoising using soft heuristic SURE thresholding and scaled noise option, on detail coefficients obtained from the decomposition at level 5 by 'sym8' wavelet.
11. Wavelet denoising using minimax thresholding at level 5 by 'db5' wavelet.
12. Smoothing Splines, presented by Reinsh (Reinsh, 1967).

The output of each algorithm was treated as a respiratory component in *IP* signal.

The calibration was performed by calculating the single coefficient from linear modeling of the volume-related reference and processed respiratory *IP* component, after detrending and mean removal (the post-processing removes the need to take into account the intercept coefficient of linear modeling). The calibration was performed for signals gained during each breathing protocols and for all three body positions. The calibration coefficients and determination coefficients of the linear model were stored.

In order to compare *TV* values, separate inspiratory and expiratory *TV* were estimated as the difference between the extremums before and after each breathing phase, *e.g.*, for inspiration,  $TV_{in}$  was calculated as the difference between the maximum found during short breathing pause after inspiration and before expiration, and the minimum found during breathing pause before that inspiration, as suggested by *Poupard et al.* (Poupard et al., 2008).

*ECG* signals were also compared for signals measured for all three body positions. However, due to the fact, that for 4 participants reference *ECG* signals were weak during sitting and standing, only those, which were recorded during supine position, were taken into account. The R points were automatically marked using simple thresholding technique.

The cardiac *IP* component was estimated as a difference between raw signal and respiratory component. We evaluated whether the possibility to extract the R points from cardiac *IP* component was linked with the equivalent of signal-to-noise ratio (*SN*, assumed as the ratio between mean absolute value of the cardiac *IP* component after mean removal, and mean absolute value of the respiratory *IP* component after mean removal as well).

All analyses were performed using MATLAB software. The processing time of the algorithms were measured with the computer processor Intel i5 (1200MHz), without any accelerations. It is worth noted, that the specific numbers are of secondary importance, the most essential is their mutual relationship.

### 3 RESULTS

Breathing phases were firstly estimated from reference signal. The sample output of the algorithm for the first participant, from 1st calibration procedure, for supine body position, is presented in the Fig. 4.

Next, we performed the calibration for all signals gained from all participants. In the Fig. 5 sample relationship between respiratory *IP* component and reference with linear model between them, are presented.

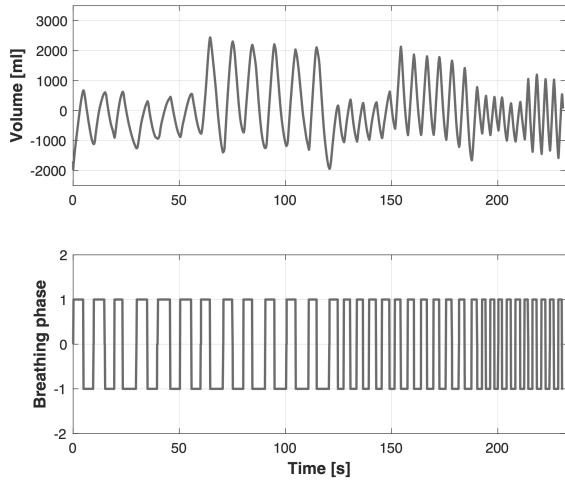


Figure 4: Sample output of the algorithm to detect breathing phases from reference *PNT* signal.

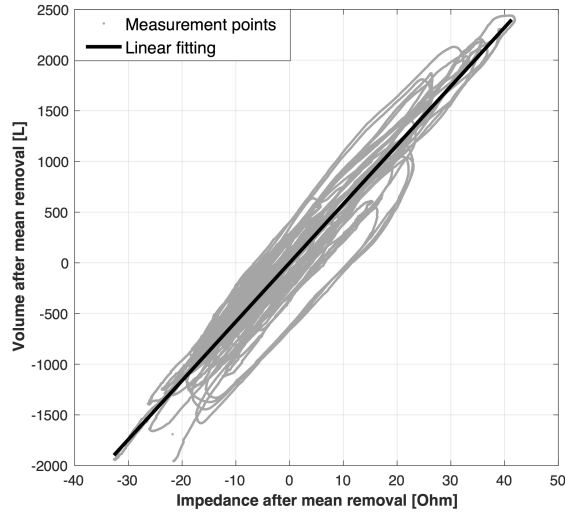


Figure 5: Sample relationship between respiratory component of impedance pneumography signal and reference, and linear calibration model.

In the Tables 2 and 3 we gathered mean determination coefficients of linear models, and mean processing times of the algorithms, respectively, depending on the calibration procedures.

Further, we used calculated calibration coefficients to evaluate the accuracy of tidal volumes, measured both for inspiration and expiration. We gathered all accuracies for both breathing phases in the Table 4, distinguishing algorithm type and calibration procedure. The accuracy is shown as absolute and relative errors. We also presented the compatibility and the Bland-Altman plots for the calculated tidal volumes, for 1st calibration procedure and for 7th algorithm. They are presented in the Fig. 6 and 7, respectively.

Table 2: The mean determination coefficient of the linear model, depending on the algorithm and calibration procedure.

Algorithm	Procedure [%]			
	1	2	3	4
1	94.2	91.1	92.2	92.1
2	95.3	91.2	92.3	92.2
3	94.4	89.6	92.0	92.0
4	82.8	82.7	90.8	90.2
5	79.5	79.9	90.1	89.5
6	90.9	88.9	91.8	91.5
7	93.3	90.6	92.1	91.9
8	93.1	90.6	92.0	91.8
9	3.7	11.4	46.8	50.2
10	91.2	89.1	91.6	91.2
11	88.7	87.2	91.6	91.1
12	92.9	87.2	91.6	91.6

Table 3: The mean processing times of the algorithm, depending on the calibration procedure.

Algorithm	Procedure			
	1	2	3	4
1 [ms]	3.4	7.1	11.4	18.3
2 [ms]	4.4	9.9	11.6	15.9
3 [ms]	5.9	11.7	13.1	19.3
4 [ms]	5.6	12.3	13.5	18.3
5 [ms]	5.5	11.6	12.5	17.3
6 [s]	0.17	1.06	1.77	3.52
7 [s]	0.16	1.06	1.70	3.73
8 [ms]	24.4	26.0	36.3	42.3
9 [s]	0.15	0.14	0.17	0.19
10 [ms]	29.9	37.6	43.5	56.1
11 [ms]	24.8	29.8	27.9	38.8
12 [s]	1.63	25.53	45.16	106.09

Then, we compared the tachograms estimated from reference *ECG* and cardiac component of *IP* signal for all subjects, for supine body position. The sample signals obtained for first subject are presented in the Fig. 8.

The comparison of the accuracy of the heart rate estimation for cardiac components derived from *IP* signal using different algorithms is presented in the Table 5.

The minimal overall error of cardiac calculations from *IP* was obtained for third algorithm.

We observed no statistically significant correspondence between the accuracy of cardiac calculations from *IP* signals, and the *SN* ratio.

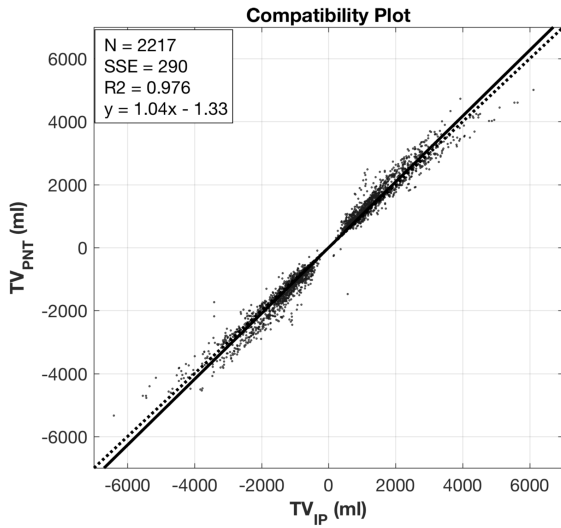


Figure 6: Compatibility plot for tidal volumes, calculated both for inspirations' and expirations' values, for all participants, for each body positions, for 1st calibration procedure and for 7th algorithm.

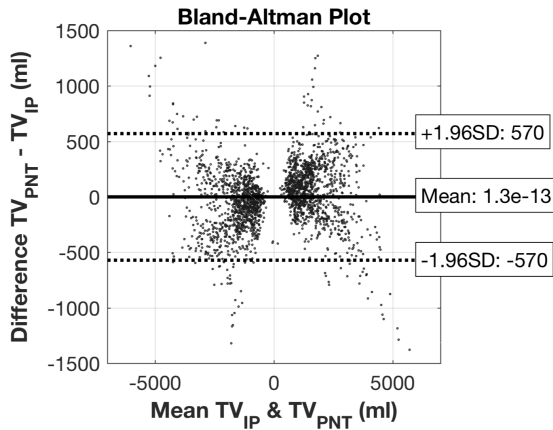


Figure 7: Bland-Altman plot for tidal volumes, calculated both for inspirations' and expirations' values, for all participants, for each body positions, for 1st calibration procedure and for 7th algorithm.

## 4 DISCUSSION

In this work various algorithms were evaluated for decomposition of the respiratory and cardiac components in *IP* signal accuracy. Among them no one seemed to be the best in every assessed aspect. Still important thing remains, what will be the best criteria for decomposition optimization.

The results showed, that from respiratory perspective moving average smoothing with short window or 7th algorithm provided the best results, however the time of operation was quite long for the second one. In cardiac analysis, moving average smoothing

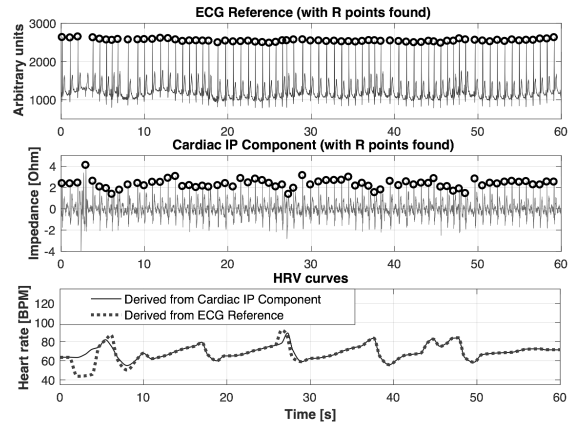


Figure 8: Sample comparison of the cardiac *IP* component with reference *ECG* signal, and the *HRV* curves derived from those signals.

with longer window appears to have the best compatibility to *ECG* reference. It seems that mixing the approaches, depending on the analyzed signal, could give the most reliable results.

The results also demonstrated, that because of the linear relationship between respiratory *IP* component and reference volume signal, there is no need to distinguish the depth and rate of breathing during calibration procedure. On the other hand, the shorter time of calibration registration allows to get higher determination coefficient of linear model, and increase the mean accuracy of tidal volume calculation.

The purpose of the testing was not to evaluate the accuracy of using calibration coefficient independently on body position; all results assumed different coefficients calculated for different positions.

There are some limitations of this study. There were only 10 participants, only males - this probably had no direct impact on the results, but it seems worth to apply the analysis in women's signals, which are quite different, e.g., due to the geometry of the chest. Further, the measurements were carried out only in static conditions, without considering motion artifacts; and there was no multi-lead *ECG* reference device. At the end, in ambulatory situations, the registrations are longer and would be more diversified, which may affect the overall accuracy.

Therefore, future plans include performing measurements during dynamic conditions, which imitate natural functioning of subjects, and then changing the way of pre-processing (particularly detrending part) from "global" approach, to the "local" one, in order to deal with non-linear and non-stationary drift of the baseline impedance.

From the analytics perspective, there is a need for further improvement and assessment of the compo-

Table 4: The comparison of tidal volume estimating accuracy, regarding algorithm type and calibration procedure; all absolute errors are in milliliters, except 9th algorithm (marked in italics), in which are in liters, and all relative errors are in percent; statistical significance is presented by \* abbreviations: A - absolute error, R - relative error,  $p$  -  $p$ -value of paired T test.

Alg.	Procedure				
	1	2	3	4	
<b>1</b>	A	214.7	240.5	251.0	165.3
	R	13.8	16.0	17.1	11.8
	$p$	0.91	0.90	0.83	0.76
<b>2</b>	A	206.0	245.7	284.2	205.7
	R	13.5	16.7	19.3	14.4
	$p$	0.74	0.77	0.77	0.71
<b>3</b>	A	238.1	278.5	338.7	273.9
	R	15.6	19.1	23.2	19.2
	$p$	0.57	0.61	0.71	0.68
<b>4</b>	A	317.9	298.9	251.9	181.2
	R	19.8	18.6	18.1	14.0
	$p$	0.91	0.94	0.88	0.84
<b>5</b>	A	343.5	311.8	264.1	200.6
	R	21.6	19.5	19.8	16.1
	$p$	0.91	0.93	0.87	0.84
<b>6</b>	A	246.8	255.5	246.4	160.7
	R	16.1	17.0	17.2	12.1
	$p$	0.96	0.94	0.83	0.75
<b>7</b>	A	223.8	243.0	247.9	161.8
	R	14.7	16.4	17.2	11.9
	$p$	0.90	0.88	0.81	0.71
<b>8</b>	A	234.3	251.2	240.1	153.0
	R	14.9	16.5	16.5	11.2
	$p$	0.99	0.99	0.88	0.80
<b>9</b>	A	<i>1.60</i>	<i>1.49</i>	<i>1.19</i>	<i>1.13</i>
	R	97.1	92.0	85.5	82.2
	$p$	0.94	0.72	0.01*	0.00*
<b>10</b>	A	246.6	258.4	248.0	162.3
	R	15.7	16.9	17.0	11.8
	$p$	0.94	0.96	0.92	0.90
<b>11</b>	A	267.9	273.1	249.3	165.5
	R	17.1	17.7	17.3	12.3
	$p$	0.92	0.94	0.92	0.89
<b>12</b>	A	309.9	320.9	379.2	317.4
	R	19.3	21.6	26.2	22.5
	$p$	0.56	0.59	0.72	0.74

nents' decomposition, e.g., using time series algorithms utilized in econometrics field.

The possibility to remove the classical *ECG* registration from ambulatory cardiorespiratory measurements in the situations, in which direct sophisticated analysis of multi-lead *ECG* signal is not necessary, has to be evaluated in the broader manner.

Table 5: The comparison of heart rate derived from cardiac *IP* components and compatibility of the shape of *HRV* curve; only the best algorithms are presented; fifth subject did not have any recognizable cardiac component, therefore was removed from presenting; abbreviations: A - absolute error [BPM], R - relative error in percent, CC - cross-correlation coefficient between *HRV* curves derived from *ECG* reference and cardiac *IP* component, SN - the equivalent of signal-to-noise ratio.

Subject		Algorithm			
		2	3	7	12
<b>1</b>	A	-0.05	-0.18	0.47	-0.16
	R	-0.1	-0.3	0.7	-0.2
	CC	0.44	0.45	0.83	0.40
	SN	0.09	0.10	0.06	0.09
<b>2</b>	A	3.91	1.26	1.68	3.70
	R	5.8	1.9	2.5	5.5
	CC	0.46	0.40	0.38	0.50
	SN	0.40	0.46	0.32	0.51
<b>3</b>	A	2.17	-1.04	-3.99	-2.53
	R	3.2	-1.5	-6.0	-3.8
	CC	0.40	0.54	0.51	0.48
	SN	0.15	0.17	0.13	0.19
<b>4</b>	A	0.66	1.38	-0.12	0.66
	R	1.1	2.3	-0.2	1.1
	CC	0.43	0.60	0.28	0.43
	SN	0.56	0.57	0.53	0.56
<b>6</b>	A	17.25	8.38	28.86	12.26
	R	32.7	15.9	54.6	23.2
	CC	-0.03	-0.09	0.09	0.01
	SN	0.34	0.42	0.26	0.43
<b>7</b>	A	0.01	0.01	0.02	0.01
	R	0.01	0.02	0.02	0.02
	CC	1.0	1.0	1.0	1.0
	SN	0.25	0.26	0.22	0.25
<b>8</b>	A	0.05	0.05	0	0.05
	R	0.1	0.1	0	0.1
	CC	0.98	0.98	1.0	0.98
	SN	0.20	0.22	0.20	0.21
<b>9</b>	A	0.02	0.03	0.02	0.02
	R	0.02	0.04	0.02	0.02
	CC	1.0	0.91	1.0	1.0
	SN	0.32	0.37	0.31	0.39
<b>10</b>	A	5.62	1.44	0.87	1.61
	R	8.6	2.2	1.3	2.5
	CC	-0.02	0.28	0.34	0.33
	SN	0.13	0.15	0.11	0.15

## 5 CONCLUSIONS

Impedance pneumography could be used to measure respiratory activity, intended primarily for ambulatory conditions. In order to get volume values, the calibration for each participant is needed. However,

short recording of free breathing, for various body positions, seemed to be enough to get the highest accuracy of tidal volume estimation.

Raw impedance signal obtained from the chest consists of both respiratory and cardiac components, the second most commonly regarded as an element to be removed. The study showed, that there is the possibility to measure and extract each component from impedance pneumography separately, with reliable accuracy, 86.5% and 97.3%, respectively for tidal volume and heart rate estimation.

Simple moving average smoothing (with 1s window for respiratory analysis, and with 1.5s window for cardiac one) were the best algorithm regarding compromise between tidal volume and heart rate accuracy, and time of processing. More sophisticated adaptive filtering also provided good accuracy, however the processing time was 100-times higher, comparing to simple methods.

Cardiac component is not equally visible in every participant, however obtained compatibility between *ECG* reference seems promising, particularly concerning ambulatory long-term measurements.

## ACKNOWLEDGEMENTS

This study was supported by the research programs of institutions the authors are affiliated with.

## REFERENCES

- Ansari, S., Ward, K., and Najarian, K. (2016). Motion Artifact Suppression in Impedance Pneumography Signal for Portable Monitoring of Respiration: an Adaptive Approach. *IEEE J. Biomed. Heal. Informatics*, 11(4):1–1.
- Barros, A. K., Yoshizawa, M., and Yasuda, Y. (1995). Filtering noncorrelated noise in impedance cardiography. *IEEE Transactions on Biomedical Engineering*, 42(3):324–327.
- Houtveen, J. H., Groot, P. F. C., and De Geus, E. J. C. (2006). Validation of the thoracic impedance derived respiratory signal using multilevel analysis. *Int. J. Psychophysiol.*, 59(2):97–106.
- Koivumaki, T., Vauhkonen, M., Kuikka, J. T., and Hakulinen, M. a. (2012). Bioimpedance-based measurement method for simultaneous acquisition of respiratory and cardiac gating signals. *Physiol. Meas.*, 33(8):1323–1334.
- Mathworks (2016). Wavelet Denoising. <http://www.mathworks.com/help/wavelet/ug/wavelet-denoising.html>. [Online; accessed 07-August-2016].
- Młyńczak, M. and Cybulski, G. (2012). Impedance pneumography: Is it possible? In *XXX Symp. Photonics Appl. Astron. Commun. Ind. High-Energy Phys. Exp. (Wilga 2012)*, volume 8454, pages 84541T–19.
- Młyńczak, M., Niewiadomski, W., Żyliński, M., and Cybulski, G. (2015). Verification of the Respiratory Parameters Derived from Impedance Pnumography during Normal and Deep Breathing in Three Body Postures. In *IFMBE Proc.*, volume 45, pages 162–165.
- Poupard, L., Mathieu, M., Sartène, R., and Goldman, M. (2008). Use of thoracic impedance sensors to screen for sleep-disordered breathing in patients with cardiovascular disease. *Physiol. Meas.*, 29(2):255–267.
- Reinsch, C. H. (1967). Smoothing by spline functions. *Numerische Mathematik*, 10(3):177–183.
- Savitzky, A. and Golay, M. J. E. (1964). Smoothing and Differentiation of Data by Simplified Least Squares Procedures. *Anal. Chem.*, 36(8):1627–1639.
- Schoenberg, I. J. (1964). Spline functions and the problem of graduation. *Proceedings of the National Academy of Sciences*, 52(4):947–950.
- Schuessler, T. F., Gottfried, S. B., Goldberg, P., Kearney, R. E., and Bates, J. H. T. (1998). An adaptive filter to reduce cardiogenic oscillations on esophageal pressure signals. *Ann. Biomed. Eng.*, 26(2):260–267.
- Seppa, V. P., Hyttinen, J., Uitto, M., Chrapek, W., and Viik, J. (2013a). Novel electrode configuration for highly linear impedance pneumography. *Biomed. Eng. / Biomed. Tech.*, 58(1):35–38.
- Seppa, V.-P., Hyttinen, J., and Viik, J. (2011). A method for suppressing cardiogenic oscillations in impedance pneumography. *Physiol. Meas.*, 32(3):337–345.
- Seppa, V. P., Uitto, M., and Viik, J. (2013b). Tidal breathing flow-volume curves with impedance pneumography during expiratory loading. In *Proc. Annu. Int. Conf. IEEE Eng. Med. Biol. Soc. EMBS*, volume 2013, pages 2437–2440.
- Seppa, V.-P., Viik, J., and Hyttinen, J. (2010). Assessment of pulmonary flow using impedance pneumography. *IEEE Trans. Biomed. Eng.*, 57(9):2277–2285.
- Wang, Z., Wu, D., Chen, J., Ghoneim, A., and Hossain, M. A. (2016). A Triaxial Accelerometer-Based Human Activity Recognition via EEMD-Based Features and Game-Theory-Based Feature Selection. *IEEE Sens. J.*, 16(9):3198–3207.
- Yasuda, Y., Umezu, A., Horihata, S., Yamamoto, K., Miki, R., and Koike, S. (2005). Modified thoracic impedance plethysmography to monitor sleep apnea syndromes. *Sleep Med.*, 6(3):215–224.